

Influences of Current Density on the Structure and Corrosion Resistance of Ceramic Coatings on ZK60 Mg Alloy by Plasma Electrolytic Oxidation

Zhaozhong Qiu, Rui Wang*, Xiaohong Wu, Yushen Zhang

School of Chemical Engineering and Technology, Harbin Institute of Technology, Heilongjiang 150001, PR China

*E-mail: wangrui001@hit.edu.cn

Received: 30 November 2012 / Accepted: 29 December 2012 / Published: 1 February 2013

Current density was a key factor of plasma electrolytic oxidation (PEO) process. It influenced the composition, morphology and corrosion resistance of ceramic coatings on ZK60 Mg alloy by plasma electrolytic oxidation in Na_2SiO_3 solution. The microstructure and composition of coatings were examined by scanning electron microscope (SEM) and X-ray diffraction (XRD), respectively. The corrosion resistance of the coatings was studied by electrochemical impedance spectroscopy (EIS) and potentiodynamic polarization techniques. The corrosion resistance of the coated samples was improved compared with that of substrate, which increases evidently by 2-3 orders after PEO treatment.

Keywords: Plasma electrolytic oxidation; Magnesium alloy ZK60; Ceramic coatings; Corrosion resistance

1. INTRODUCTION

Magnesium alloys are becoming increasingly attractive for potential use in a wide range of structural applications, including in the automotive industry, because of their low density, good machinability, excellent damping capacity and favorable recycling capability [1].

However, a critical limitation for the extensive application of magnesium alloys is their susceptibility to corrosion, especially in chloride environments[2–4]. There are numerous surface modification techniques available to protect magnesium alloys, such as chemical conversion coating, electrochemical plating, gas-phase deposition processes, laser surface alloying, organic coating and plasma electrolytic oxidation [5–8]. Amidst which the plasma electrolytic oxidation treatment is becoming increasingly popular in recent years. [9–13]. The surface properties of PEO coatings such as wear resistance, corrosion resistance, heat resistance, electrical insulation, adhesion to substrate can be

considerably improved [14–18]. In this study, the influences of current density on the composition, morphology and corrosion resistance of ceramic coatings on ZK60 Mg alloy by PEO are researched.

2. EXPERIMENTAL

2.1. Preparation of PEO coatings

Polished rectangular sample (with dimensions 25mm×20mm×2mm) made of ZK60 Mg alloy (mass fraction: Zn 5.5%, Zr 0.5%, balance Mg) was used as the substrate material in this study. They were ground successively with 180, 600, 1000 and 2000 grit emery sheets and cleaned with acetone before the PEO treatment. A homemade pulsed bipolar electrical source with power of 5 kW was used for plasma electrolytic oxidation of samples in a water-cooled electro-bath made of stainless steel, which also served as the counter electrode. The reaction temperature of the electrolytes during the processing was kept at 20±2°C with a cooling water flow. The PEO process equipment used was similar to the one presented by Matthews' group [19]. An aqueous electrolyte was prepared from a solution of sodium silicate (10g/L), potassium hydroxide (5g/L), sodium citrate(3g/L) and sodium tungstate (1g/L). The electronic power frequency was fixed at 1000 Hz. The duty ratios of both pulses were both equal to 40%. The whole process was carried out for 6 min under the current density of 3, 6, 9 and 12 A/dm², respectively. After PEO treatment, the coated samples were rinsed with deionized water and dried in the air.

2.2. Analysis of composition and structure of PEO coatings

The phase composition of the coating was investigated by means X-ray diffraction (XRD), using a Cu K α source. The surface morphology of the prepared coating was observed using scanning electron microscopy (SEM; SU-8000). Electrochemical impedance spectroscopy (EIS) and potentiodynamic polarization experiments were performed through Princeton-4000 electrochemical analyzer. EIS was used to analyze the corrosion nature of the coatings prepared under different current density during immersion in 3.5% NaCl solution. Each sample was mounted by paraffin with 1cm² surface exposed. The signal amplitude of EIS was 10 mV over frequency ranged between 0.01 and 10 kHz. Potentiodynamic polarization was used to investigate pitting corrosion properties at a scan rate of 1 mV/s, with a scanning range from -100 mV to +100 mV of open circuit potential. The corrosion potential and the corrosion current density were obtained through the linear analysis of Tafel approximation. All electrochemical measurements were performed with a conventional three electrodes system of coated samples as working electrode, a platinum plate as auxiliary electrode and Ag/AgCl(sat KCl) as reference electrode. All experiments were carried out at room temperature.

3. RESULTS AND DISCUSSION

3.1. Voltage-time response

The galvanostatic dependencies of positive voltage vs. time on PEO with different current densities were shown in Fig. 1, in which the current density was 3, 6, 9 and 12 A/dm², respectively. After the PEO process began, the current density was kept constantly at a certain value, while the instantaneous variation of voltage was recorded every 10s during the plasma electrolytic oxidation process. As shown in Fig. 1, the positive voltage increased as the current density increasing. In these curves, four stages could be identified [20].

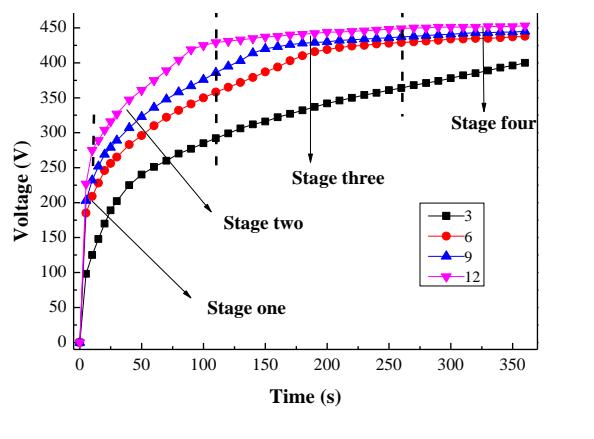


Figure 1. Voltage-time response for PEO coatings produced under different current densities.

The voltage increased evidently with time, the trend was almost a straight line up, there was no spark and only some tiny oxygen bubbles could be seen on the sample surface in the first stage, which indicated that magnesium alloy substrate began to dissolve and a thin passive film formed on the surface of the magnesium alloy. Once the voltage exceeded the breakdown voltage, stage II started, With the increase of voltage, a lot of small micro-sparks appeared and oxygen evolution also became vigorous on the surface of magnesium alloy. We took the (d) curve for example. The breakdown voltage in the alkaline sodium silicate electrolyte was found to be 227 V. During the second stage, the cell voltage increased continually with the processing of the PEO. White micro-sparks became more phonic and the oxygen evolution became more vigorous than those in the previous stage after about 110 seconds treatment. All this indicated that the anodizing process got into stage III. When the voltage was up to 450 V, the process entered the IV stage, the rate of voltage increase continued to slow down as the voltage reaching a more stable state. The micro-sparks were larger than those in the III stage and the sound of the PEO process was very harsh, the number of the sparks decreased and it happened to arise continuous sparking at the edge of the sample.

3.2. Phase composition of the coatings

The X-ray diffraction patterns of the oxide coating formed in the same electrolyte with variations of the current densities were showed in Fig. 2(a-d). It was apparent that the XRD pattern of the PEO coating was mainly constituted with MgO phase and there was also a little amount of MgSiO₃ phase, regardless of the variations in the current density.

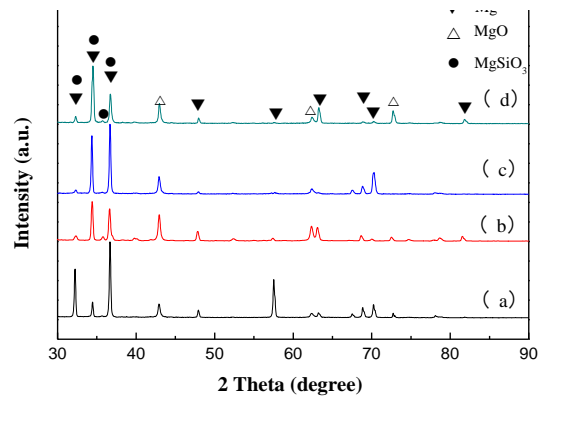


Figure 2. XRD patterns of the ceramic coatings produced under different current densities: (a) 3A/dm²; (b) 6A/dm²; (c) 9A/dm² (d)12 A/dm².

3.3. Morphologies of the coatings

Fig.3. displayed the surface morphologies of the PEO coatings obtained under different current densities. The surface of the specimen PEO coating contained more or less a small level of micro pores density and some micro cracks. The surface containing considerable craters were due to discharge energy through the channels during the PEO process and oxygen bubbles generated by decomposition of OH⁻ [21] on the anodic electrode (reaction (1) thrown out of micro-arc discharge channels [22]).



It should be noted that there were micro-cracks on the surface which were caused by thermal stress due to rapid solidification of molten oxide by the electrolyte acting as a coolant. Moreover, the lower Pilling–Bedworth ratio (PBR) of magnesia (PBR is the ratio of the volume of the elementary cell of a metal oxide to the volume of the elementary cell of the corresponding metal) was also the main reason for cracks and high porosity of PEO films on magnesium alloys [23].

The pores of different shapes were observed to be distributed all over the surface. It was also apparent that the number of the pores was decreasing, while the diameter of the pores was increased significantly with adding current density. The increasing current density accelerated the discharging

energy led to the increased product mass by a single pulse, which contributed to the enlarged pore sizes after the discharged channels were cooled. As the discharge intensity increasing continuously, the accumulated production mass of oxide increased and induced the enlargement of grain size gradually, and overlapped the pores nearby.

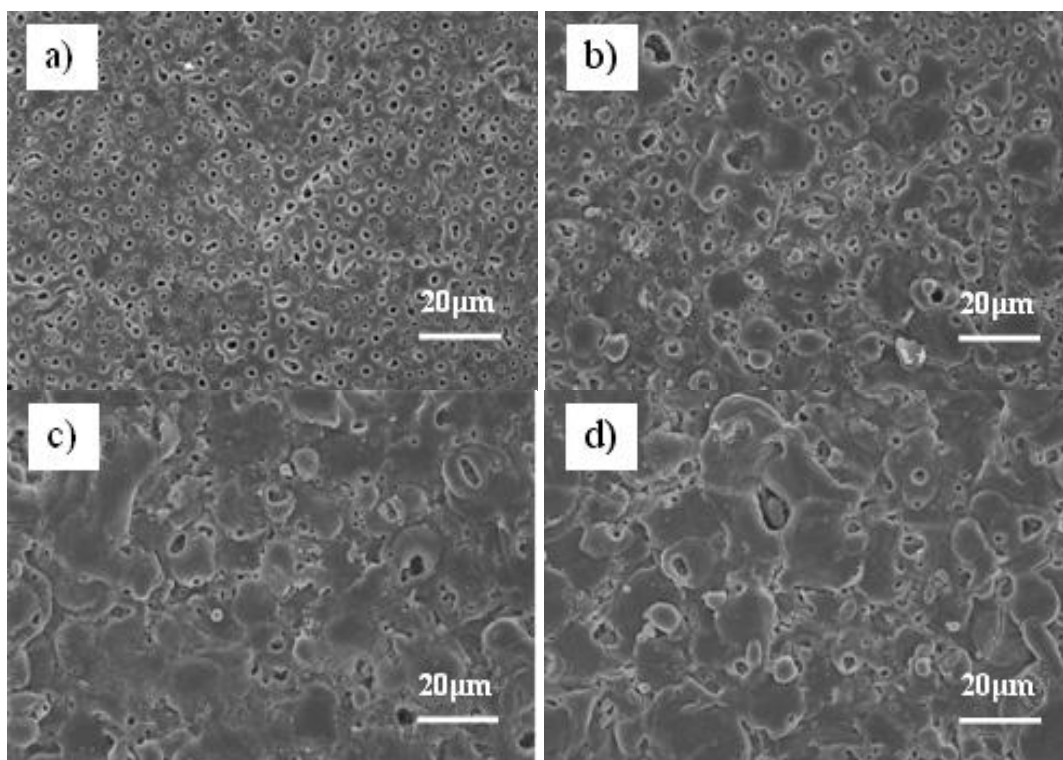


Figure 3. Surface morphologies of the ceramic coatings produced under different current densities: (a) 3A/dm^2 ; (b) 6A/dm^2 ; (c) 9A/dm^2 , (d) 12A/dm^2 .

3.3 Corrosion behavior of the coatings

3.3.1 Electrochemical impedance spectroscopy characteristics

The EIS characteristics of magnesium alloy with uncoated sample and coated samples were measured in 3.5% NaCl solution and the results were shown in Fig.4. EIS equivalent circuit for magnesium electrode with PEO coatings was proposed as shown in Fig.5.

From the equivalent circuit, the impedance of the measured system between reference electrode (Ag/AgCl(sat KCl)) and working electrode (PEO coating) consisted of three parts: electrolyte, outer porous layer and inner compact layer. The equivalent circuit (shown in Fig. 5) consisted of the solution resistance (R_s), two constant phase element of coating (CPE), the outer porous layer resistance (R_p) of the PEO coating parallel with constant phase element (CPE) Q_p and the inner compact layer resistance (R_b) of the PEO coating in parallel with Q_b [24]. the capacity element was expressed as follows[25,26],

$$Z_{CPE} = 1/[T(j\omega)^n] \tag{2}$$

Where T is the admittance constant, *j* is imaginary number, ω is the angular frequency, and *n* is the CEP exponent ranging between 0 and 1. The case *n* = 1 describes an ideal capacitor while the case *n* = 0 describes a pure resistor. When the value of 0.5 implies that the circuit reflected the Warburg impedance[27].

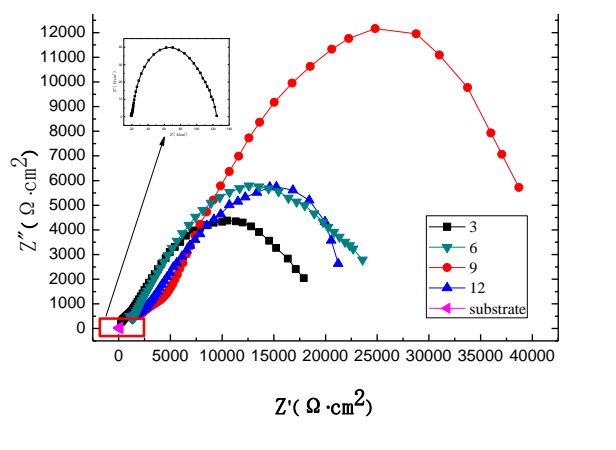


Figure 4. Nyquist diagrams for different sample in 3.5 wt% NaCl solution

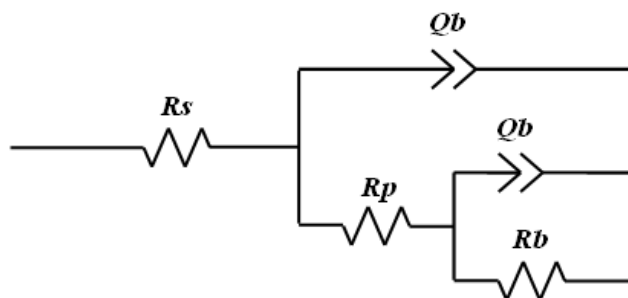


Figure 5. Equivalent circuit related to the EIS plots of the coating obtained by different current density

With the Nyquist plots based on the equivalent circuit model shown in Fig. 5, an excellent fit was made between the experimental data and iterated result. The results of the fitting parameters for simulative EIS spectra of the coated samples obtained under different current densities were shown in Table 1. It could draw conclusions from the EIS results that the corrosion resistance of magnesium electrodes was increased evidently by 2-3 orders after PEO treatment due to the formation of ceramic PEO coatings on magnesium alloy ZK60 substrate. In addition, compared to the resistance of the inner compact layer, the resistance value of the outer layer was too small to contribute to the corrosion protection of the magnesium alloy[28]. The fitting results showed that polarization resistance ($R_p + R_b$)

reached up to $4.89 \times 10^4 \Omega \text{cm}^2$ and the values of resistances of outer porous layer (R_p) and inner compact layer (R_b) of the sample fabricated at 9 A/dm^2 were higher than that of the other three samples prepared at 3, 6, and 12 A/dm^2 . The different EIS behavior (corrosion resistance) of these PEO coatings could be due to their different structure. As the current density was increased, the pores became fewer and smaller which could slow down the penetration rate of electrolyte into the PEO coating[29].

Table 1. The values of the electrical elements of the equivalent circuit shown in Fig. 5 fitting EIS data of Fig. 4

Sample (A/dm ²)	R_s	Q_p-Y_0 ($\Omega^{-1} \text{s}^{-n}/\text{cm}^2$)	n_p	R_p	Q_b-Y_0 ($\Omega^{-1} \text{s}^{-n}/\text{cm}^2$)	n_b	R_b
3	259.1	1.172E-6	0.5886	1396	6.389E-6	0.5315	1.93E4
6	1068	6.892E-7	0.7036	2114	4.604E-6	0.5094	2.38E4
9	1700	1.893E-6	0.5476	3861	7.062E-7	0.6267	4.51E4
12	853.1	3.533E-6	0.8003	3053	9.59E-6	0.5576	2.31E4

3.3.2 Potentiodynamic polarization

The potentiodynamic polarization curves of the PEO coating and bare sample in 3.5% NaCl solution were shown in Fig. 6 and the associated electrochemical data were listed in Table2. These data clearly shown that the corrosion resistances of these samples with and without PEO coatings were evidently different. The bare sample exhibited a corrosion current density of $1.05 \times 10^{-4} \text{ A/cm}^2$ with an associated corrosion potential $-1.565 \text{ vs. Ag/AgCl(sat KCl)}$.

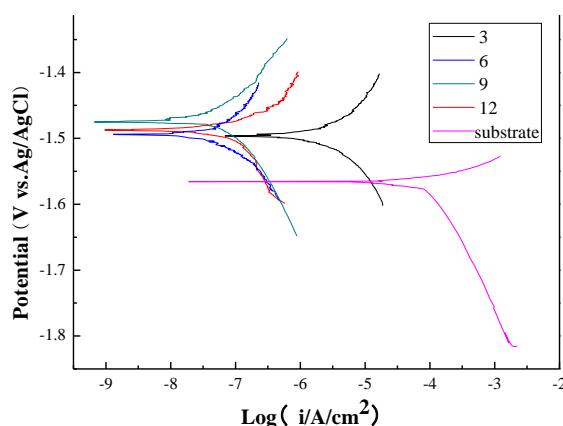


Figure 6. Potentiodynamic polarization curves of samples with different current density in the 3.5 wt% NaCl solution.

In contrast with bare magnesium alloy ZK60, the samples with PEO coatings had more positive corrosion potential and much more negative corrosion current density, which indicated that corrosion resistance of magnesium alloy ZK60 had been improved obviously by PEO treatment and consider the low corrosion current density and/or the high corrosion potential led to a good corrosion resistance[30].

As to these samples with PEO coatings prepared under different current densities, adding the current density to 9 A/dm², the corrosion potential of the coatings increased, while the corrosion current density decreased. As current density growth continuing, the corrosion current density was decreased from 1.30×10⁻⁷ A/cm² to 4.43×10⁻⁷ A/cm², which illustrated that the corrosion rate of increase was slowed down. Therefore, the sample prepared under the current density of 9 A/dm² was the best one, which was consistent with the result of EIS.

Table 2. Corrosion current Density and Corrosion Potential of Substrate and coated Samples Produced Under different current density

Sample (A/dm ²)	Corrosion current density (A/cm ²)	Corrosion potential (V)
Substrate	1.05×10 ⁻⁴	-1.565
3	8.7×10 ⁻⁶	-1.496
6	2.27×10 ⁻⁷	-1.492
9	1.30×10 ⁻⁷	-1.474
12	4.43×10 ⁻⁷	-1.487

4. CONCLUSION

We studied the influence of current density to the composition, morphology, and corrosion resistance of the coatings prepared on the surface of ZK60 magnesium alloy using the plasma electrolytic oxidation technique. Corrosion resistance of the coatings could be tremendously improved by adjusting the current density. The fitting results showed that polarization resistance ($R_p + R_b$) reached up to 4.89×10⁴ Ωcm². Estimated from potentiodynamic polarization curves, the corrosion current density of the sample of 9 A/dm² increased three orders compared to the bare sample exhibits a corrosion current density of 1.05×10⁻⁴ A/cm², the corrosion current density was decreased to 1.30×10⁻⁷ A/cm². The corrosion resistance of the coated samples was improved dramatically after PEO treatment.

ACKNOWLEDGEMENT

The authors thank the National key Laboratory of Vacuum and Cryogenics Technology and Physics (Project No. 9140C550201060C55) for the financial support for this work.

References

1. K. Kubota, M. Mabuchi, K. Higashi, *J. Mater. Sci.* 34 (1999) 2255.
2. G. Song, A. Atrens, D. St. John, X. Wu, *J. Nairn, Corros. Sci.* 39 (1997) 1981.

3. N. Birbilis, M.A. Easton, A.D. Sudholz, S.M. Zhu, M.A. Gibson, *Corros. Sci.* 51(2009) 283.
4. G. Song, A. Atrens, *Adv. Eng. Mater.* 9 (2007) 117.
5. K. Z. Chong and T. S. Shih, *Mater. Chem. Phys.*, 80[1] 191–200 (2003).
6. J. Chen, D. H. Bradhurst, S. X. Dou, and H. K. Liu, *J. Alloys Compd.*, 280 [1–2] 290–293 (1998).
7. G. Reiners and M. Griepentrog, *Surf. Coat. Technol.*, 76–77 [2] 809–814 (1995).
8. K. T. Rie and J. Wöhlle. *Surf. Coat. Technol.*, 112 [1–3] 226–229 (1999).
9. J.E. Gray, B. Luan, *J. Alloys Compd.* 336 (2002) 88.
10. A.L. Yerokhin, X. Nie, A. Leyland, A. Matthews, S.J. Dowey, *Surf. Coat. Technol.* 122 (1999) 73.
11. C. Blawert, W. Dietzel, E. Ghali, G. Song, *Adv. Eng. Mater.* 8 (2006) 511.
12. P. Gupta, G. Tenhundfeld, E.O. Daigle, D. Ryabkov, *Surf. Coat. Technol.* 201(2007) 8746.
13. X. Zhong, Q. Li, J. Hu, Y. Lu, *Corros. Sci.* 50 (2009) 2304.
14. R.H.U. Khan, A. Yerokhin, X. Li, H. Dong, A. Matthews, *Surf. Coat. Technol.* 205(2010) 1679.
15. J.S. Cai, F.H. Cao, L.R. Rong, J.J. Zheng, J.Q. Zhang, C.N. Cao, *Appl. Surf. Sci.* 257(2011) 3804.
16. Y. Chen, X. Nie, D.O. Northwood, *Surf. Coat. Technol.* 205 (2010) 1774.
17. M. Shokouhfar, C. Dehghanian, A. Baradaran, *Appl. Surf. Sci.* 257 (2011) 2617.
18. K.C. Kung, T.M. Lee, J.L. Chen, T.S. Lui, *Surf. Coat. Technol.* 205 (2010) 1714.
19. A.L. Yerokhin, X. Nie, A. Leyland, A. Matthews, S.J. Dowey. *Surf. Coat. Technol.* 122 (1999) 73–93.
20. C. X. Ma, Y. Lu, P. P. Sun, Y. Yuan, X. Y. Jing, M. L. zhang. *Surf. Coat. Technol.* 2011, 206, 287-294.
21. A. K. Vijh, *Corros. Sci.*, 11 [6] 411–417 (1971)
22. A.K. Sharma, R. Uma Rani, A. Malek, K.S.N. Acharya, M. Muddu, S. Kumar, *Met. Finish.* 94 (1996) 16–27.
23. X. Zhou, G.E. Thompson, P. Skeldon, G.C. Wood, K. Shimizu, H. Habazaki, *Corros. Sci.* 41 (1999) 1599–1613.
24. P. B. Srinivasan , J. Liang, R.G. Balajee, C. Blawert, M. Stormer, W. Dietzel, *Appl. Surf. Sci.* 256(2010) 3928–3935
25. C. H. Hsu, F. Mansfeld, *Corros. Sci.*, 57 (2001) 747.
26. J. R. Macdonald, *Annals of Biomedical Engineering*, 1992, 20[3], 289–305
27. S.C. Chung, J.R. Cheng, S.D. Chiou, *Corros. Sci.* 42 (2000) 1249.
28. H.F. Guo, M.Z. An, H.B. Huo, S. Xu, L.J. Wu, *Appl. Surf. Sci.* 252 (2006) 7911.
29. P.B. Su, X.H. Wu, Z. H. Jiang, Y. Guo, *Int. J. Appl. Ceram. Technol.*, 8 [1] 112–119 (2011)
30. Y.G. Ko, S. Namgung, D.H. Shin, *Surf. Coat. Technol.* 205 (2010) 2525e2531.